

ADDITIVE MANUFACTURING (AM) AND NANOTECHNOLOGY: PROMISES AND CHALLENGES

Olga S. Ivanova¹, Christopher B. Williams², Thomas A. Campbell^{1}*

1. Institute for Critical Technology and Applied Science (ICTAS), Virginia Tech, Blacksburg, Virginia, 24061, USA
 2. Department of Mechanical Engineering & Department of Engineering Education, Virginia Tech, Blacksburg, Virginia, 24061, USA
- * Corresponding Author, tomca@vt.edu, 540-231-8359

REVIEWED, August 17 2011

Abstract

The narrow choice of materials used in Additive Manufacturing (AM) remains a key limitation to more advanced systems. Nanomaterials offer the potential to advance AM materials through modification of their fundamental material properties. In this paper, the authors provide a review of available published literature in which nanostructures are incorporated into AM printing media as an attempt to improve the properties of the final printed part. Specifically, we review the research in which metal, ceramic, and carbon nanomaterials have been incorporated into AM technologies such as stereolithography, laser sintering, fused filament fabrication, and three-dimensional printing. The purpose of this article is to summarize the research done to date, to highlight successes in the field, and to identify opportunities that the union of AM and nanotechnology could bring to science and technology.

Introduction

Additive Manufacturing (AM) is a group of emerging technologies that create objects from the bottom-up by adding material one cross-sectional layer at a time [1]. For the past three decades, researchers and engineers have focused on improving old and creating new techniques, as well as developing novel materials.

AM methods have several advantages over traditional manufacturing techniques. First, AM offers “design freedom” for engineers; because of its additive approach, it is possible to build geometries that cannot be fabricated by any other means. Moreover, it is possible with AM to create functional parts without the need for assembly. Also, AM offers reduced waste; minimal use of harmful chemicals, such as etching and cleaning solutions; and the possibility to use recyclable materials.

Despite these design and environmental advantages, the adoption of AM as a means for fabricating end-use components has historically been dampened by the technologies’ narrow selection of available materials. The majority of materials used presently by modern AM techniques are proprietary polymers. There are also possibilities to use some metals (such as steel alloys and titanium) and ceramics. While there are different types of materials that can be used in AM, the material properties are typically not as strong as their conventionally manufactured counterparts due to the anisotropy caused by the layer-by-layer approach. Therefore, options within these materials genres are usually limited to applications of models for form/fit testing, functional testing, presentation models, prototypes and non-load bearing products. Furthermore, variations in build process parameters, and in some AM processes,

ambient conditions, can result in variations between parts built on different machines of the same AM technology. Overcoming these issues will require advances in both process control approaches and material selection.

The integration of nanotechnology with AM has the potential to both complement existing techniques and to create wholly new nanocomposites; it is thus a promising approach to alleviating some of the technologies' limitations. "Nanotechnology is science, engineering, and technology conducted at the nanoscale, which is about 1 to 100 nanometers" [2]. When shrinking the size scale from macro to nano, or bulk to molecule, materials can change their fundamental properties. For example, at the nanoscale, objects can exhibit unique optical [3-6], thermal [7], and electrochemical [8-10] properties that differ from the properties of the bulk material or molecules. These properties strongly depend on the size and the shape of nanostructures [11, 12]. There are also a wide variety of nanomaterials, including carbon nanotubes (CNTs), nanowires (NWs), buckyballs, graphene, metal nanoparticles (NPs), and quantum dots (QDs). All these materials possess unique characteristics that allow applications in areas such as sensing [13-15], separation [16], plasmonics [17-19], catalysis [20-25], nanoelectronics [26-28], therapeutics [29-31], and biological imaging and diagnostics [32-38]. *Thus, the addition of nanomaterials to AM printing media could enable the creation of entirely new composites possessing unique properties and lead to expansion of application areas of AM.*

Published research combining AM and nanomaterials thus far is limited. Nevertheless, articles have shown that the introduction of inorganic nanostructures such as CNTs, metal NPs, and ceramics can significantly affect sintering characteristics and final mechanical properties of the printed parts. This literature review summarizes the work performed to date in the area of incorporating nanomaterials into AM and describes the effects of the addition of nanostructures on the physical properties of the final printed part. We conclude with a discussion of challenges and opportunities remaining in the union of AM and nanotechnology.

Metal Nanoparticles

Metal nanoparticles (NPs) are of great interest to researchers because their optical, thermal and electrochemical properties depend significantly on their size. Metal NPs can be synthesized with different shapes – spheres, cubes, rods – depending on the process. Figure 1-A shows the photographs of silver and gold nanoparticle solutions synthesized by chemical reduction method in the presence of citrate ions [39, 40]. Figure 1-B represents a typical SEM (Scanning Electron Microscopy) image of the spherical Ag nanoparticles ($d=10-15$ nm) deposited on an electrode surface. Metal NPs have found applications in sensing, catalysis, bio-imaging, drug delivery, and microelectronics.

Recently metal NPs have been utilized for the purposes of improving the sintering characteristics and creation of new printing materials for AM. One of the first reports on using metal nanoparticles for AM is by Crane, *et al.*, in 2006 [41]. Crane used iron NPs (diameter = 7 to 10nm) to improve the sintering quality of steel parts created by 3D printing (3DP). The test specimens were printed using traditional binder and a steel powder ranging from 63 to 90 μ m in diameter. Different approaches for infiltration of NPs were tested, such as multiple applications of nano-binders, the rate of drying, drying under a magnetic field, and the use of oxidized and unoxidized NPs. It was found that the addition of a nano-binder to the printed parts decreased deflection and shrinkage. Figure 2 shows the comparison of creep deflection of two printed parts

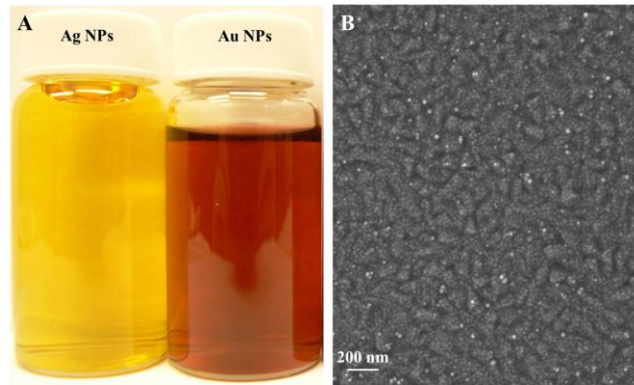


Figure 1. (A) Photographs of Ag and Au nanoparticle solutions. (B) SEM image of the Ag NPs deposited on a Glass/ITO electrode surface.

during sintering, the first with nano-iron treatment and the second without nano-iron treatment. The deflection of the part treated with nano-iron was reduced by 95% and shrinkage was reduced by 60%. Crane suggests that the application of the nano-binder multiple times decreased the deflection of the final parts by enlarging the bonds between bigger particles and curing the cracks formed after the sintering process.

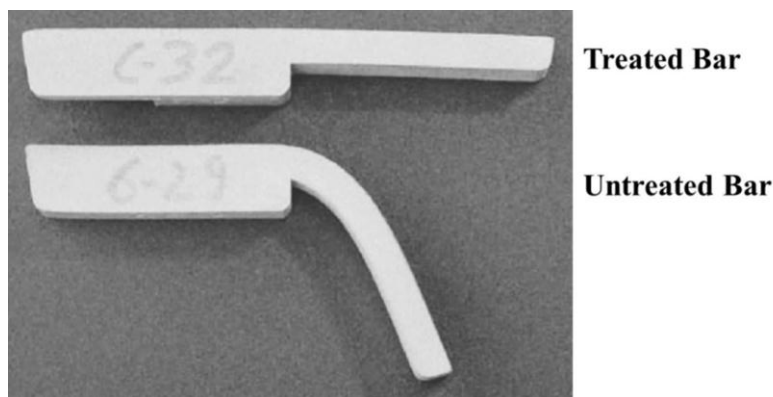


Figure 2. Comparison of deflection of stainless steel bars with and without nano-iron treatment. Treated bar received four applications and was dried under a magnetic field. Ref. [41]

Bai, *et al.*, [42] added silver NPs (diameter = 30 nm) directly into a binder solution to create a silver NP suspension for 3DP. It was shown that the nanosilver suspension could be sintered at 300°C. Low sintering temperatures of metal nanoparticles are due to the thermodynamic size effect [7]. The quality of the parts printed with nanobinder and with traditional binder was compared. It was demonstrated that the addition of Ag NPs improved the sintering characteristics of the final part. Parts printed with nanobinder showed less distortion and shrinkage compared to a pure binder system.

Use of highly concentrated Ag NPs suspension for fabrication of microelectrodes using Omnidirectional Printing was shown by Ahn, *et al.* [43]. Ag nanosuspensions with solid loadings of >70% were produced by concentrating the NPs with ethanol and centrifugation. These highly concentrated NP inks were then used for fabrication of Ag microelectrodes. It was

possible to use nozzles with a diameter as narrow as 1 μm to print silver nanosuspensions (70% loading) without clogging. Printing of planar and flexible microelectrodes, and also multilayered and arched architectures, was achieved using these inks (Figure 3). Electrical resistivity and effects of mechanical bending on the electrical performance of fabricated microelectrodes were tested. Electrical resistivity of these electrodes decreased with an increase in annealing temperature and was close to the value for bulk silver when annealed at 250°C. Printed electrodes demonstrated steady electrical response for at least 750 bending cycles.

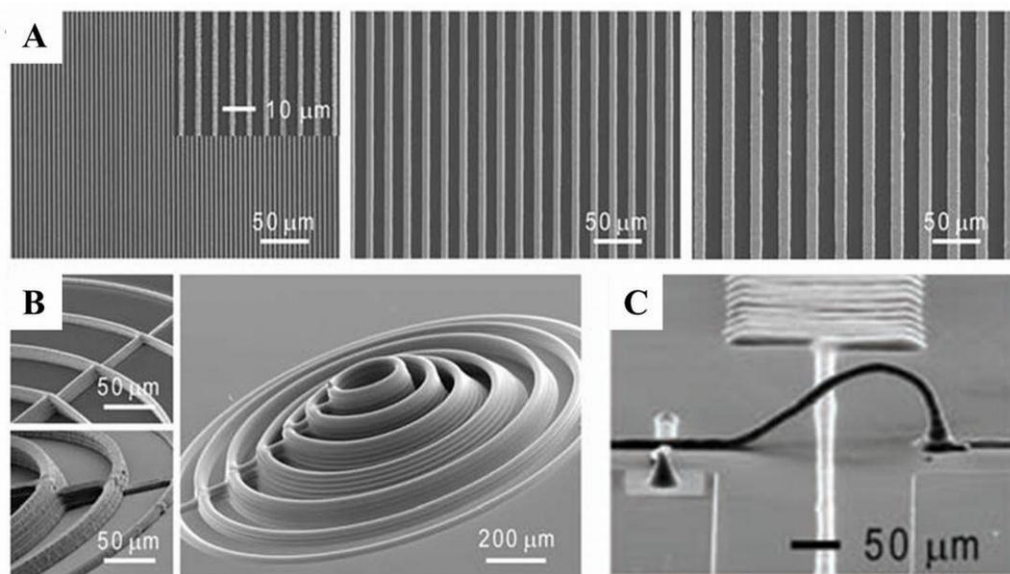


Figure 3. (A) SEM images of planar arrays of silver microelectrodes patterned with 1- (left), 5- (center), and 10-mm (right) nozzles. (B) SEM images of multilayer silver microelectrodes patterned with 5- (top left), 10- (bottom left), and 30-mm (right) nozzles. (C) a silver interconnect arch printed over an electrode junction. Ref. [43]

These examples show that the addition of metal NPs can significantly affect sintering characteristics of the final parts, decreasing their shrinkage and distortion. Also, highly concentrated metal NP inks are promising materials for the fabrication of microelectrodes and microconnectors; they could find use in microelectronics, solar cells, batteries, *etc.*

Carbon Nanotubes and Nanofibers

Carbon nanotubes (CNTs) are allotropes of carbon. The structure of CNTs is cylindrical; each carbon atom has three neighbors, as in graphite. CNTs are considered as rolled-up graphene sheets (graphene is a one-atom-thick sheet of graphite). There are three primary CNT forms – armchair, zig-zag, and chiral – as shown in Figure 4; characterization of CNTs can be challenging and may require new instruments [44]. Carbon nanotubes are among the strongest and stiffest materials known [45, 46], and they possess unique electrical and thermal conductivities [47-50]. CNTs have been consequently used as additives to polymers to improve mechanical, thermal, and electrical properties [51, 52]. They have found applications in hydrogen storage, field emission devices, sensors, and scaffolds for damaged nerve regeneration,

etc. [53-55]. Here we describe work performed with CNTs as additives to the materials for Stereolithography, Laser Sintering and Direct Writing.

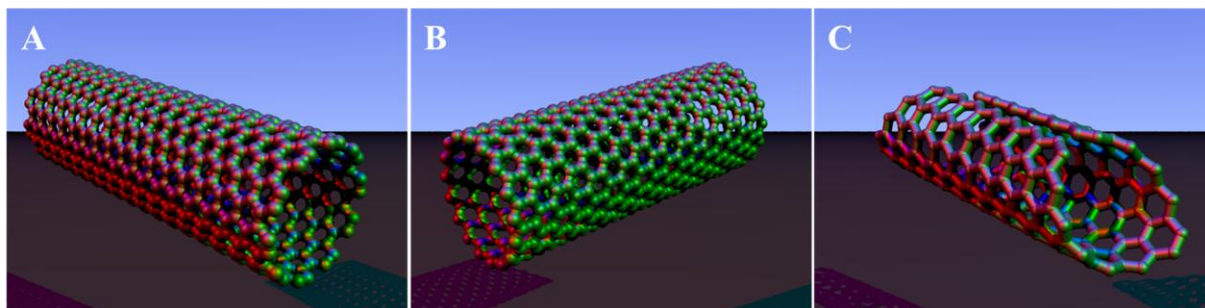


Figure 4. Single walled CNTs structures: (A) armchair, (B) zig-zag, and (C) chiral.

Sandoval, *et al.* [56, 57] used multiwalled carbon nanotubes (MWCNTs) with an average diameter of 30nm and lengths in the range of 5 to 20 μ m as an additive to stereolithography (SL) resin. Results showed that the addition of MWCNTs increase tensile stress and fracture stress by \sim 5.7% and \sim 26%, respectively, for 0.025 wt.% MWCNT resin compared to unfilled resin. When 0.1 wt.% MWCNT resin was used, tensile stress increased by \sim 7.5%, while fracture stress increased by \sim 33% compared to pure resin. While mechanical performance of specimens was improved, the addition of MWCNTs resulted in more brittle material compared to pure resin. The specimens fabricated with MWCNTs showed a decrease in elongation at break of \sim 28%. Also, it was noted that increasing the loading of the MWCNTs from 0.025% to 0.1% did not significantly affect mechanical properties and brittleness.

Athreya, *et al.* [58] used nanosized carbon black (CB) powder blended with Nylon-12 powder for Laser Sintering (LS). Their work was focused on finding optimal printing conditions of the nanocomposites. Flexural modulus of Nylon-12/CB composites was found to be lower than pure Nylon-12, depending on scan speed and laser power. The “optimum” parameters were found to be 4W laser power with 30 in/sec scan speeds. Also, it was observed that some portion of particles do not melt during the SLS process, but they remain in their original form in the final printed part. Electrical conductivity of final parts was five orders of magnitude higher for parts printed from Nylon-12/CB composite compared to pure Nylon-12.

Athreya, *et al.* [59] also compared Nylon-12/CB parts made by LS with objects made by extrusion-injection molding. As in [58], Nylon-12/CB composites were compared with pure Nylon-12. It was found that parts prepared by LS have lower tensile modulus than those prepared using molding. Pure Nylon-12 parts prepared by molding had higher impact strength compared to parts fabricated by LS. The addition of CB to the Nylon-12 resulted in a decrease in impact strength for both LS and molding parts. Notable results were observed in the dispersion of CB within the polymer after printing. It was shown that LS led to formation of large agglomerates of CB within the polymer, whereas parts prepared by the extrusion molding demonstrated uniformly distributed sub-100nm aggregates. Furthermore, the porosity of parts produced by LS was \sim 10%, while parts fabricated by extrusion had porosity of $<$ 5%.

Goodridge, *et al.*, [60] used carbon nanofibers (CNF) as additives to Polyamide-12 for LS. Printing material was prepared by melt mixing 3 wt.% CNF with Polyamide-12. Three systems were compared: 1) as-supplied Polyamide-12 powder, 2) CNF/polyamide-12 (melt mixing), and 3) Polyamide-12 with all the steps of preparation of the CNF/polyamide-12 mixture, but without CNF (Neat Polyamide-12). Figure 5 shows the photographs of the powder

bed and printed parts for the three materials. Sintered parts prepared using CNF/Polyamide-12 and pure Polyamide-12/melt mixing had a rough surface compared to as-received Polyamide-12. Storage modulus (demonstration of elastic response) and loss modulus (viscous response) were determined for all three systems. Parts printed with as-supplied Polyamide-12 demonstrate the highest moduli compared to the other two systems. Parts prepared using CNF showed 22% and 15% higher storage modulus and loss modulus, respectively, compared to Polyamide-12/melt mixing. SEM analysis showed that CNFs are well dispersed in the polymer after the LS procedure. Overall, the addition of CNFs improved the mechanical properties of sintered parts compared to similarly prepared Polyamide-12, but the resulting parts were not smooth.

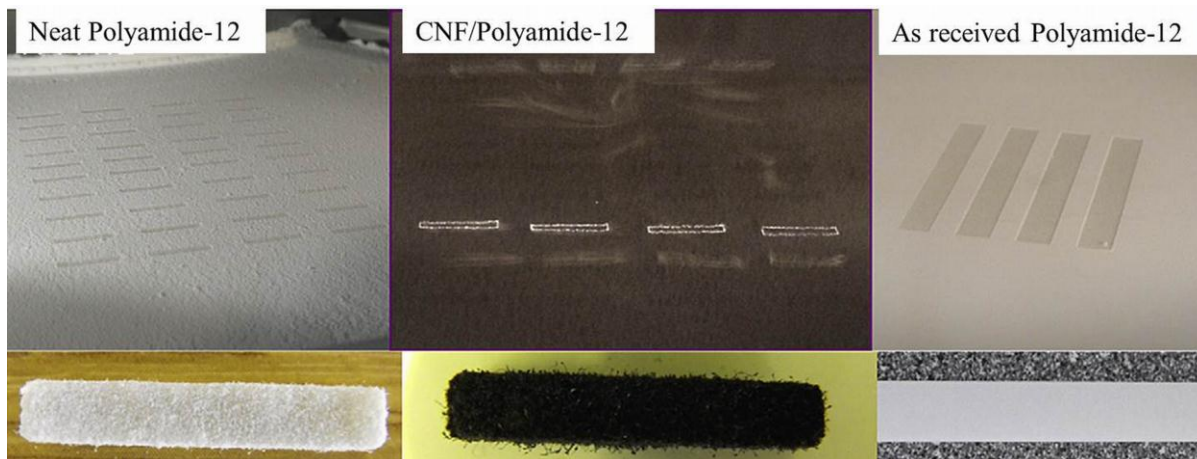


Figure 5. Photographs of the powder bed (top) and fabricated parts (bottom) using three different materials as indicated. Ref. [60]

Similar studies were performed by Lao, *et al.* [61]. They used MWCNT melt-blended with Polyamide-11. Injection and compression molded specimens were prepared for characterization of their mechanical and thermal properties. Tensile strength and tensile modulus increased with increasing MWCNT loading, while elongation at break decreased with increasing MWCNT loadings. Thermo-gravimetric analysis (TGA) analysis showed that thermal stability increases with increase in MWCNT loading. At 50% mass loss, decomposition temperature increased from 439°C for pure Polyamide-11 to 488°C for 7 wt.% MWCNT/Polyamide mixture. The electrical resistivity of polymer nanocomposites decreased with increase of MWCNT loading.

Yildirim, *et al.*, [62] demonstrated the excellent biocompatibility of Single Walled Carbon Nanotubes (SWCNT) – alginate composites for application as a tissue scaffolds. Tissue scaffolds were prepared by Freeform Fabrication technique (an analog of FFF), using 1 wt.% SWCNT mixed with alginate as a printing material. Figure 6 shows the morphology of printed three-dimensional scaffolds with and without SWCNT. SWCNTs were evenly dispersed on the alginate surface, but the printed surface was rough compared to pure alginate. Mechanical testing showed higher tensile stress and tensile modulus for alginate/SWCNT composites, but smaller elongation at break values compared to pure alginate. More importantly, it was demonstrated that alginate/SWCNT composites are promising materials for tissue growth. Scaffolds printed using SWCNTs showed a constant cell proliferation rate for up to one week

and the number of cells on day seven was six times higher than on day one; the rate of proliferation is higher than pure alginate scaffolds.

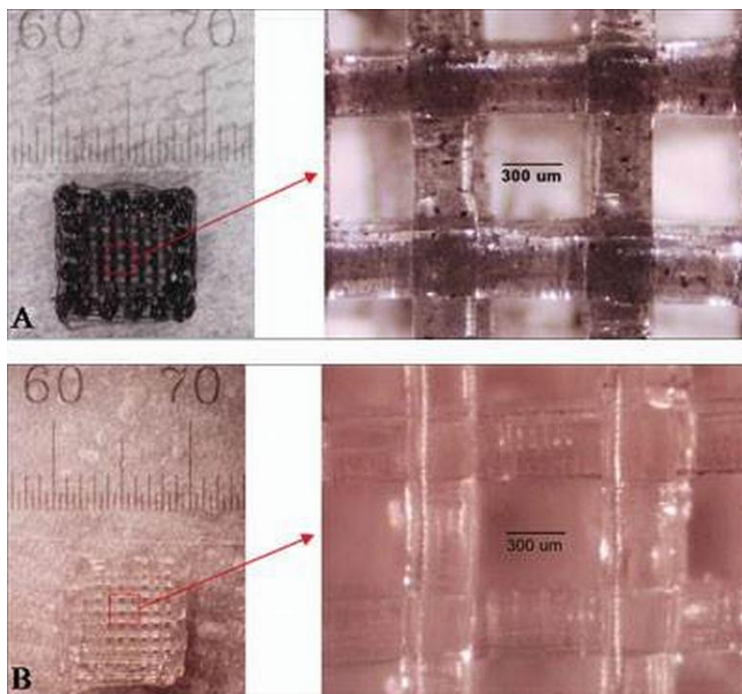


Figure 6. Photographs (left side) and micrographs (right side) of fabricated 3D scaffolds using (A) SWCNTs/Alginate composite and (B) pure alginate. Ref. [62]

These experiments demonstrate that the addition of carbon nanotubes to SL resins and LS materials can improve mechanical properties of final parts. In all cases, tensile stress and fracture stress increased with the addition of carbon nanomaterials, while elongation at break decreased. The addition of carbon nanomaterials also increased electrical conductivity of the final parts. Finally, it was shown that carbon nanotube–alginate tissue scaffolds can improve the rate of cell proliferation during culture tests.

Ceramic and Semiconductor Nanoparticles

Ceramics are usually inorganic, non-metallic materials such as oxides, carbides and nitrides. As in the case of metal NPs, the size of ceramic NPs plays a crucial role, especially on sintering temperature. Some ceramic materials such as SiO_2 and TiO_2 show semiconducting properties. A semiconductor is a material with electrical conductivity in-between a conductor and an insulator. Such materials are characterized by conduction and valence energy bands, which are separated by a known energy range (band gap). The band gap affects the semiconductor properties, such as optical and electrical properties. By altering the size of semiconductor nanoparticles, one can change the band gap and modify the properties of the material. Extensively studied semiconductor nanoparticles include cadmium chalcogenides (Quantum Dots) [63, 64]. However, other types of semiconductor nanoparticles have been synthesized and investigated [65-69]. Figure 7 shows the photographs of colloidal solutions of Cd free Quantum Dots. These materials have found application in optoelectronic devices [70],

solar cells [71], bio-imaging [72, 73], and labeling [74]. Here we describe the effects of the addition of ceramic and semiconductor nanoparticles on mechanical properties of parts fabricated by AM.

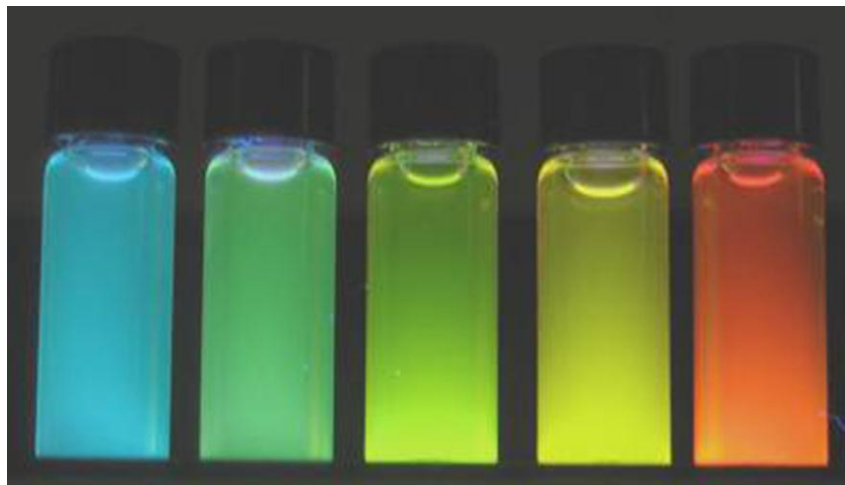


Figure 7. Brightly glowing vials of highly luminescent, water soluble quantum dots produced by the new NIST microwave process span a wavelength range from 500 to 600 nm. Credit: NIST (National Institute of Standards and Technology).

Chung, *et al.* [75] used Nylon-11 loaded with silica NPs in LS to create Functionally Graded Material (FGM) composite components. FGM materials combine different composition and properties within a single component to optimize performance of that component. Silica loadings in Nylon-11 investigated were 0, 2, 4, 6 and 10 wt.%. The particle size of Nylon-11 powder was 106 to 150 μ m, while the size of silica NPs was \sim 15nm. Adjustment of printing parameters led to part density of $>90\%$ for different silica loadings. Transmission electron microscope (TEM) analysis confirmed a homogeneous distribution of silica particles inside the polymer. Mechanical tests showed that with increase of silica loading, the parts become stiffer (with an increase in tensile modulus), but also more brittle (with a decrease in tensile strain at break). It is expected that there is a critical composition at which these characteristics reverse these trends.

Cai, *et al.* [76] demonstrated Direct Writing construction of three-dimensional meshes from TiO₂ – vaseline composites. Vaseline was loaded with 0, 2.5, 5, 7.5, and 10 wt.% of TiO₂ NPs (diameter = 21nm); ink properties were investigated; 3D scaffolds were fabricated; and mechanical performance of printed scaffolds was tested. Creep and recovery tests showed that inks with low NP content (0-5 wt.%) form structures that easily damage and don't recover, while inks with high NP loading demonstrated a tendency toward lower deformation and increased elastic properties. Fabricated inks showed an excellent ability to construct 3D structures. An increase in NP content reduced rod bending and caused shrinking and folding. Scaffolds produced on the flexible substrate exhibited an ability to preserve their shape after repeated bending and stretching.

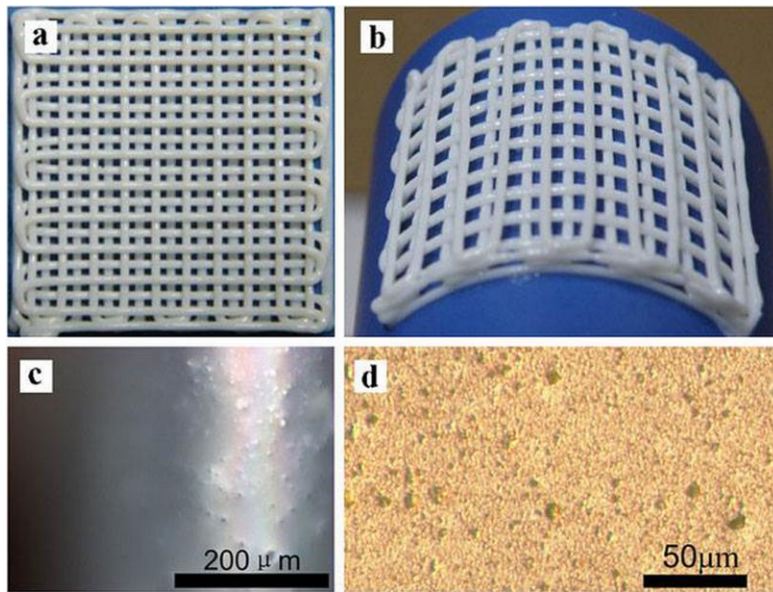


Figure 15. Images of assembled structures on different scale: (a) a four-layer scaffold piled by perpendicular rods with diameter of 500 μm and inter-rod distance of 2 mm in a 20 mm \times 20 mm square, (b) bending of the formed structure, (c) agglomeration of nanoparticles at the rod's surface, (d) magnified image of nanoparticles doped ink. Ref. [76]

Semiconductor nanoparticles were used in SL to influence the final mechanical characteristics of the fabricated parts by Duan *et al.* [77]. The addition of TiO_2 NPs (diameter=30nm) to the photosensitive resin showed promising results for improving the mechanical properties of fabricated parts. NP loadings from 0.1 to 5.0 wt.% were used. Viscosity of fabricated resins increased with increasing NP content. Properties of the final parts were studied extensively on 0.25 wt.% NP loading. The addition of TiO_2 NPs improved the mechanical properties of the final part; tensile strength increased by 89%, tensile modulus increased by 18%, flexural strength increased by 6%, and hardness increased by 5%. All these parameters indicate the improvement of plasticity of fabricated parts. Additionally, application of NPs improved thermal stability of the fabricated parts.

The Lewis group [78] used BaTiO_3 NPs (diameter=60nm) coated with poly (acrylic acid) to fabricate inks with high (>45%) solid loadings for direct writing. Experiments showed that the addition of NPs leads to an increase in shear stress and elastic modulus by one order of magnitude as the result of fluid-to-gel transition. This transition was performed using mono- or divalent salt species. It was demonstrated that the nature of salt used for fluid-to-gel transition greatly affects the elastic modulus. Elastic modulus was approximately two orders of magnitude higher in the case when divalent salt was used. Successful demonstration of printing of 2D and 3D structures with feature sizes of $\sim 30\mu\text{m}$ and $\sim 100\mu\text{m}$ was performed.

Experimental demonstration of the adjustment of the properties of printed parts by surface modification of NPs was offered by Zheng, *et al.* [79]. Al_2O_3 nanoparticles (diameter=60nm) were used in combination with polystyrene (PS) for LS. Three compositions were studied: pure PS, Al_2O_3 /PS mixture, and Al_2O_3 /PS core-shell particles produced by emulsion polymerization. Sintering of Al_2O_3 /PS core-shell particles led to formation of a

compact structure, while $\text{Al}_2\text{O}_3/\text{PS}$ mixture developed highly porous surface with numerous voids. Encapsulating NPs into the polymer matrix led to uniform dispersion of the NPs in the matrix, while NPs mixed with PS tended to form aggregates. Mechanical properties of all three materials were investigated. It was shown that impact strength and tensile strength increased (300% and 50%, respectively) for $\text{Al}_2\text{O}_3/\text{PS}$ core-shell specimens, compared to $\text{Al}_2\text{O}_3/\text{PS}$ mixture and pure PS. $\text{Al}_2\text{O}_3/\text{PS}$ core-shell samples were more ductile and demonstrated higher toughness.

The potential use of nanocomposite scaffolds for bone tissue engineering was demonstrated by Duan, *et al.* [80]. Calcium phosphate (Ca-P) and carbonated hydroxyapatite (CHAp) NPs were incorporated into poly(hydroxybutyrate-co-hydroxyvalerate) (PHBV) and poly(L-lactic acid) (PLLA), respectively. The size of calcium NPs varied from 10 to 30 nm. These nanocomposites were used to fabricate tissue scaffolds using the LS technique. Mechanical properties, such as compressive strength and modulus, of nanocomposite scaffolds were higher than those of pure polymers in dry environment. Biological evaluation of fabricated scaffolds was carried out with human osteoblast-like cells (SaOS-2). After three days of culture growth, almost no dead cells were found on all four types of scaffolds, thus indicating high cell viability of the fabricated scaffolds. Cell proliferation was enhanced in the case of Ca-P/PHBV scaffolds compared to pure PHBV, while no difference was observed in cell proliferation between CHAp/PLLA and pure PLLA scaffolds. After seven days, cultured cells were well attached and spread over the scaffold surface for all four types of materials.

In summary, the use of semiconductor and ceramic nanoparticles as additives to LS, SL, and Direct Writing materials has shown promising results in enhancing mechanical properties of final printed parts. Fabrication of FGM components and tissue scaffolds has been also successfully demonstrated. Biodegradable ceramic nanostructures can be successfully applied in bone tissue engineering.

Summary of Published Literature

Table 1 summarizes the state of the art on the inclusion of nanomaterials in AM as of this writing.

Table 3. Summary of published literature of AM with nanomaterials.

Nanomaterial AM Method	Metal Nanoparticles	Carbon Nanotubes and Nanowires	Semiconductor and ceramics Nanoparticles
Stereolithography (SL)	N/A	Increase tensile stress and fracture stress, more brittle parts, decrease elongation at break [56, 57]	TiO ₂ - increase tensile strength and modulus, flexural strength and hardness . Improved thermal stability [77].
Laser Sintering (LS)	N/A	<ul style="list-style-type: none"> • Flexural modulus lower, parts less dense, electrical conductivity significantly enhanced [58]. • Decrease in impact strength, formation of aggregates within a polymer [59]. • Improved mechanical properties, good distribution within polymer, but rough final surface [60]. 	<ul style="list-style-type: none"> • Silica – parts stiffer but more brittle [75]. • Al₂O₃/PS – enhance sintering characteristics, formation of compact structure, increase impact strength and tensile strength, samples more ductile and tougher [79]. • Ca-P and CHAp – improved compressive strength and modulus, high cell viability [80].
3D Printing (3DP)	<ul style="list-style-type: none"> • Fe for Steel parts – decrease creep deflection, and shrinkage [41]. • Ag for Ag parts - less distortion and shrinkage. Improved sintering [42]. 	N/A	N/A
Fused Filament Fabrication (FFF) (Robocasting, Direct Writing, or Onidirectional Printing)	Ag NPs ink - microelectrodes (layered and arches), flexible substrate, steady electrical response for at least 750 bending cycles [43].	Increase in tensile stress and tensile modulus, decrease in elongation at break. Increase in cell proliferation rate [62].	<ul style="list-style-type: none"> • TiO₂ – reduce rod bending, but promote shrinking and folding. On flexible substrate, preserve shape after repeated bending [76]. • BaTiO₃ – increase shear stress and elastic modulus of inks [78].

Challenges in AM and Nanomaterials

There are several challenges inherent in the merger of AM and nanomaterials. The most important issue that needs to be resolved is agglomeration of the nanomaterials in printing media when working with extrusion methods, 3DP, and Stereolithography. Agglomeration of the particles most likely will lead to loss of their unique properties (i.e., nanomaterial will behave as a bulk). To overcome this issue, functionalization of the nanomaterials with organic linker molecules is required. Linkers can keep particles away from each other, even when embedded into the printing media. Solving this problem will lead to the design of wholly new nanocomposite inks that can improve the properties of the final parts and preserve the unique characteristics of the nanomaterial embedded into the printing material.

When using SL in combination with nanomaterials, one should find suitable nanomaterials for a given wavelength of the UV light source. The cure depth of the SL can be affected by the presence of nanomaterials due to their ability to absorb the UV light. Much research will be required to overcome this challenge. Experiments on finding the ideal wavelength that will solidify the polymer without being affected by the presence of the nanostructures may be necessary.

Published work on inclusion of nanomaterials into LS, in some cases, showed that porosity of the final printed parts is higher compared to parts printed without nanomaterials. This could be due to the different nature of materials used (carbon black and Nylon-12, or Silica NPs and Nylon-11, etc.). The synthesis of core-shell nanostructures, where the core consists of the nanomaterial of interest and the shell consists of the printing material, can improve the density of the final parts [79]. Resolving this issue will provide new printing materials that possess unique properties – electrical and thermal conductivities, hardness – while simultaneously yielding nanocomposites as dense as nanostructure-free printed parts.

3DP and extrusion processes also have their challenges, when combined with nanomaterials. The most significant issue is nozzle clogging when high loadings of nanomaterials are used. This could be due to the formation of aggregates within the printing material. More experimental work is required to determine the ideal composition of nano-inks, that could flow freely through nozzles.

Conclusions

This review provides an overview of the work done to date to incorporate nanostructures into Additive Manufacturing (AM). The addition of metal nanoparticles generally decreases sintering temperatures, improves part density, and decreases shrinkage and distortion of printed parts. Metal nanoparticles embedded into polymer materials can also provide improved electrical conductivity in fabricated objects. Incorporation of carbon nanotubes in printing media offers a potential route to improving mechanical properties of the final parts and to increasing electrical and thermal conductivities. The addition of carbon nanotubes in bio-scaffolds can yield excellent enhancement of cell proliferation. Adding semiconductor and ceramic nanoparticles to printing media can lead to improvements in mechanical properties of the final parts. Ceramic nanoparticles can be effectively used for bone tissue engineering.

Despite these early successes, challenges in the application of nanomaterials to AM are nevertheless numerous. Each of the AM methods described has its own inherent limitations (nozzle clogging, aggregation within printing media, rough surface finish of printed parts *etc.*)

when nanoparticles are applied with the respective printing media. Overcoming these design boundaries may require the development of new instrumentation for successful AM with nanomaterials.

It is shown that there are many opportunities in the marriage of AM and nanotechnology. By leveraging the tunable properties of nanostructures, we can expand the material properties, and thus applications, of printed components. Moreover, it may be possible with AM-produced nanocomposites to create objects with graded material properties by varying the nanostructure loadings during a part's synthesis. Combining multiple nanomaterials in the same AM part would then allow us to move from simple to more complex printed objects such as fuel cells, batteries, solar cells, *etc.* Recent advancements in nano-biomaterials could also further enable the printing of replacement organs and bone. Again, these forthcoming directions will require not only a greater focus on the development of new materials for existing AM systems, but they also may necessitate the development of wholly new AM approaches.

Overall, we find promising results have been published in the application of nanomaterials and AM, yet significant work remains to fully harness their inherent potential. The research community has much work to do, but the rewards could be great in the integration of Additive Manufacturing with nanotechnology.

Acknowledgements

The authors gratefully acknowledge funding from the Institute for Critical Technology and Applied Science (ICTAS) at Virginia Tech for postdoctoral associate support of one of the authors (O.I.).

References

1. *Standard Terminology for Additive Manufacturing Technologies*, 2010, ASTM International West Conshohocken, PA.
2. <http://www.nano.gov/>. *What is Nanotechnology?* ; Available from: <http://www.nano.gov/>.
3. Alivisatos, A.P., *Semiconductor Clusters, Nanocrystals, and Quantum Dots*. *Science*, 1996. **271**(5251): p. 933-937.
4. Mulvaney, P., *Surface Plasmon Spectroscopy of Nanosized Metal Particles*. *Langmuir*, 1996. **12**(3): p. 788-800.
5. Katz, D., et al., *Size-Dependent Tunneling and Optical Spectroscopy of CdSe Quantum Rods*. *Phys. Rev. Lett.* , 2002. **89**(8): p. 0868011-0868014.
6. Jain, P.K., et al., *Noble Metals on the Nanoscale: Optical and Photothermal Properties and Some Applications in Imaging, Sensing, Biology, and Medicine*. *Accounts Chem. Res.* , 2008. **41**(12): p. 1578-1586.
7. Buffat, P. and J.-P. Borel, *Size Effect on the Melting of Gold Particles*. *Phys. Rev. A*, 1976. **13**: p. 2287-2298.
8. Sardar, R., et al., *Gold Nanoparticles: Past, Present, and Future*. *Langmuir*, 2009. **25**(24): p. 13840-13851.
9. Ivanova, O.S. and F.P. Zamborini, *Size-Dependent Electrochemical Oxidation of Silver Nanoparticles*. *J. Am. Chem. Soc.* , 2010. **132**: p. 70-72.

10. Ivanova, O.S. and F.P. Zamborini, *Electrochemical Size Discrimination of Gold Nanoparticles Attached to Glass/Indium-Tin-Oxide Electrodes by Oxidation in Bromide-Containing Electrolyte*. *Anal. Chem.*, 2010. **82**: p. 5844-5850.
11. Daniel, M.-C. and D. Astruc, *Gold Nanoparticles: Assembly, Supramolecular Chemistry, Quantum-Size-Related Properties, and Applications toward Biology, Catalysis, and Nanotechnology*. *Chem. Rev.*, 2004. **104**: p. 293-346.
12. Burda, C., et al., *Chemistry and Properties of Nanocrystals of Different Shapes*. *Chem. Rev.*, 2005. **105**: p. 1025-1102.
13. Rosi, N.L. and C.A. Mirkin, *Nanostructures in Biodiagnostics*. *Chem. Rev.*, 2005. **105**: p. 1547-1562.
14. Haick, H., *Chemical Sensors Based on Molecularly Modified Metallic Nanoparticles*. *J. Phys. D: Appl. Phys.*, 2007. **40**: p. 7173-7186.
15. Liu, S. and Z. Tang, *Nanoparticle Assemblies for Biological and Chemical Sensing*. *J. Mater. Chem.*, 2010. **20**: p. 24-35.
16. Liu, F.-K., *Analysis and Applications of Nanoparticles in the Separation Sciences: A Case of Gold Nanoparticles*. *J. Chromatogr. A*, 2009. **1216**: p. 9034-9047.
17. Eustis, S. and M.A. El-Sayed, *Why Gold Nanoparticles are More Precious than Pretty Gold: Noble Metal Surface Plasmon Resonance and Its Enhancement of the Radiative and Nonradiative Properties of Nanocrystals of Different Shapes*. *Chem. Soc. Rev.*, 2006. **35**: p. 209-217.
18. Love, S.A., B.J. Marquis, and C.L. Haynes, *Recent Advances in Nanomaterial Plasmonics: Fundamental Studies and Applications*. *Appl. Spectrosc.*, 2008. **62**(12): p. 346A-362A.
19. Uechi, I. and S. Yamada, *Photochemical and Analytical Applications of Gold Nanoparticles and Nanorods Utilizing Surface Plasmon Resonance*. *Anal. Bioanal. Chem.*, 2008. **391**: p. 2411-2421.
20. Crooks, R.M., et al., *Dendrimer-Encapsulated Metal Nanoparticles: Synthesis, Characterization, and Applications to Catalysis*. *Accounts Chem. Res.*, 2001. **34**(3): p. 181-190.
21. Serp, P., M. Corrias, and P. Kalck, *Carbon Nanotubes and Nanofibers in Catalysis*. *Appl. Catal. A-Gen.*, 2003. **253**: p. 337-358.
22. Kolmakov, A. and M. Moskovits, *Chemical Sensing and Catalysis by One-Dimensional Metal-Oxide Nanostructures*. *Annu. Rev. Mater. Res.*, 2004. **34**: p. 151-180.
23. Narayanan, R. and M.A. El-Sayed, *Catalysis with Transition Metal Nanoparticles in Colloidal Solution: Nanoparticle Shape Dependence and Stability*. *J. Phys. Chem. B*, 2005. **109**: p. 12663-12676.
24. Chen, M. and D.W. Goodman, *Catalytically Active Gold: From Nanoparticles to Ultrathin Films*. *Accounts Chem. Res.*, 2006. **39**: p. 739-746.
25. Corma, A. and H. Garcia, *Supported Gold Nanoparticles as Catalysts for Organic Reactions*. *Chem. Soc. Rev.*, 2008. **37**: p. 2096-2126.
26. Feldheim, D.L. and C.D. Keating, *Self-Assembly of Single Electron Transistors and Related Devices*. *Chem. Soc. Rev.*, 1998. **27**: p. 1-12.
27. Lu, W. and C.M. Lieber, *Nanoelectronics from the Bottom Up*. *Nat. Mater.*, 2007. **6**: p. 841-850.

28. Sgobba, V. and D.M. Guldi, *Carbon Nanotubes - Electronic/Electrochemical Properties and Application for Nanoelectronics and Photonics*. Chem. Soc. Rev., 2009. **38**: p. 165-184.
29. Sonvico, F., et al., *Metallic Colloid Nanotechnology, Applications in Diagnosis and Therapeutics*. Curr. Pharm. Design, 2005. **11**: p. 2091-2105.
30. Boisselier, E. and D. Astruc, *Gold Nanoparticles in Nanomedicine: Preparation, Imaging, Diagnostics, Therapies and Toxicity*. Chem. Soc. Rev., 2009. **38**: p. 1759-1782.
31. Park, K., et al., *New Generation of Multifunctional Nanoparticles for Cancer Imaging and Therapy*. Adv. Funct. Mater. , 2009. **19**: p. 1553-1566.
32. Michalet, X., et al., *Quantum Dots for Live Cells, in Vivo Imaging, and Diagnostics*. Science, 2005. **307**: p. 538-544.
33. Jain, P.K., I.H. El-Sayed, and M.A. El-Sayed, *Au Nanoparticles Target Cancer*. Nano Today, 2007. **2**(1): p. 18-29.
34. Murphy, C.J., et al., *Chemical Sensing and Imaging With Metallic Nanorods*. Chem. Comm., 2008: p. 544-557.
35. Murphy, C.J., et al., *Gold Nanoparticles in Biology: Beyond Toxicity to Cellular Imaging*. Accounts Chem. Res., 2008. **41**(12): p. 1721-1730.
36. Smith, A.M., et al., *Bioconjugated Quantum Dots for in Vivo Molecular and Cellular Imaging*. Adv. Drug Deliver. Rev. , 2008. **60**: p. 1226-1240.
37. Kostarelos, K., A. Bianco, and M. Prato, *Promises, Facts and Challenges for Carbon Nanotubes in Imaging and Therapeutics*. Nat. Nanotechnol., 2009. **4**: p. 627-633.
38. Tong, L., et al., *Gold Nanorods as Contrast Agents for Biological Imaging: Optical Properties, Surface Conjugation and Photothermal Effects*. Photochem. Photobiol. , 2009. **85**: p. 21-32.
39. Jana, N.R., L. Gearheart, and C.J. Murphy, J. Phys. Chem. B, 2001. **105**: p. 4065-4067.
40. Pyatenko, A., M. Yamaguchi, and M. Suzuki, *Synthesis of Spherical Silver Nanoparticles with Controllable Sizes in Aqueous Solutions*. The Journal of Physical Chemistry C, 2007. **111**(22): p. 7910-7917.
41. Crane, N.B., et al., *Improving Accuracy of Powder-Based SFF Processes by metal Deposition from a Nanoparticle Dispersion* Rapid Prototyping J., 2006. **12**(5): p. 266-274.
42. Bai, J.G., K.D. Creehan, and H.A. Kuhn, *Inkjet Printable Nanosilver Suspensions for Enhanced Sintering Quality in Rapid Manufacturing*. Nanotechnology, 2007. **18**: p. 185701-185705.
43. Ahn, B.Y., et al., *Omnidirectional Printing of Flexible, Stretchable, and Spanning Silver Microelectrodes*. Science, 2009. **323**: p. 1590-1593.
44. Campbell, T.A. and K.D. Henry, *Carbon Nanotube Nanometrology System*, U.S. Patent, Editor 2009, ADA Technologies, Inc.: USA.
45. Yu, M.-F., et al., *Strength and Breaking Mechanism of Multiwalled Carbon Nanotubes Under Tensile Load*. Science, 2000. **287**: p. 637-640.
46. Jensen, K., et al., *Buckling and Kinking Force Measurements on Individual Multiwalled Carbon Nanotubes*. Phys. Rev. B, 2007. **76**: p. 195436-195440.
47. Lu, X. and Z. Chen, *Curved Pi-Conjugation, Aromaticity, and the Related Chemistry of Small Fullerenes (<C60) and Single-Walled Carbon Nanotubes*. Chem. Rev., 2005. **105**: p. 3643-3696.

48. Sinha, S., et al., *Off-Axis Thermal Properties of Carbon Nanotube Films*. J. Nanopart. Res. , 2005. **7**: p. 651-657.
49. Pop, E., et al., *Thermal Conductance of an Individual Single-Wall Carbon Nanotube Above Room Temperature*. Nano Lett. , 2006. **6**(1): p. 96-100.
50. Takesue, I., et al., *Superconductivity in Entirely End-Bonded Multiwalled Carbon Nanotubes*. Phys. Rev. Lett., 2006. **96**: p. 057001-057004.
51. Coleman, J.N., U. Khan, and Y.K. Gun'ko, *Mechanical Reinforcement of Polymers Using Carbon Nanotubes*. Adv. Mater., 2006. **18**(6): p. 689-706.
52. Wang, C., et al., *Polymers Containing Fullerene or Carbon Nanotube Structures*. Prog. Polym. Sci. , 2004. **29**(11): p. 1079-1141.
53. Andrews, R., et al., *Multiwall Carbon Nanotubes: Synthesis and Application*. Accounts Chem. Res., 2002. **35**: p. 1008-1017.
54. Baughman, R.H., A.A. Zakhidov, and W.A.d. Heer, *Carbon Nanotubes - the Route Toward Applications*. Science, 2002. **297**: p. 787-792.
55. Zanello, L.P., et al., *Bone Cell Proliferation on Carbon Nanotubes*. Nano Lett., 2006. **6**(3): p. 562-567.
56. Sandoval, J.H. and R.B. Wicker, *Functionalizing Stereolithography Resins: Effects of Dispersed Multi-Walled Carbon Nanotubes on Physical Properties*. Rapid Prototyping J., 2006. **12**(5): p. 292-303.
57. Sandoval, J.H., et al., *Nanotailoring Photocrosslinkable Epoxy Resins with Multi-Walled Carbon Nanotubes for Stereolithography Layered Manufacturing*. J. Mater. Sci., 2007. **42**: p. 156-165.
58. Athreya, S.R., K. Kalaitzidou, and S. Das, *Processing and Characterization of a Carbon Black-Filled Electrically Conductive Nylon-12 Nanocomposites Produced by Selective Laser Sintering*. Mater. Sci. Eng. A 2010. **527**: p. 2637-2642.
59. Athreya, S.R., K. Kalaitzidou, and S. Das, *Mechanical and Microstructural Properties of Nylon-12/Carbon Black Composites: Selective Laser Sintering Versus Melt Compounding and Injection Molding*. Compos. Sci. Technol., 2011. **71**: p. 506-510.
60. Goodridge, R.D., et al., *Processing of a Polyamide-12/Carbon Nanofibre Composite by Laser Sintering*. Polym. Test., 2011. **30**: p. 94-100.
61. Lao, S.C., et al. *Polyamide II-Carbon Nanotubes Nanocomposites: Processing, Morphological, and Property Characterization*. in *Twenty-First International SFF Symposium - An Additive Manufacturing Conference*. 2010. Austin, TX, USA.
62. Yildirim, E.D., et al., *Fabrication, Characterization, and Biocompatibility of Single-Walled Carbon Nanotube-Reinforced Alginate Composite Scaffolds Manufactured Using Freeform Fabrication Technique*. J. Biomed. Mater. Res. B: Appl. Biomater., 2008. **87**(2): p. 406-414.
63. Dabbousi, B.O., et al., *(CdSe)ZnS Core-Shell Quantum Dots: Synthesis and Characterization of a Size Series of Highly Luminescent Nanocrystallites*. J. Phys. Chem. B, 1997. **101**: p. 9463-9475.
64. Gerion, D., et al., *Synthesis and Properties of Biocompatible Water-Soluble Silica-Coated CdSe/ZnS Semiconductor Quantum Dots*. J. Phys. Chem. B, 2001. **105**: p. 8861-8871.
65. Li, L., et al., *Highly Luminescent CuInS₂/ZnS Core/Shell Nanocrystals: Cadmium-Free Quantum Dots for In Vivo Imaging*. Chem. Mater. , 2009. **21**: p. 2422-2429.

66. Pons, T., et al., *Cadmium-Free CuInS₂/ZnS Quantum Dots for Sentinel Lymph Node Imaging with Reduced Toxicity*. ACS Nano, 2010. **4**(5): p. 2531-2538.
67. Yong, K.-T., et al., *Synthesis of Ternary CuInS₂/ZnS Quantum Dot Bioconjugates and Their Applications for Targeted Cancer Bioimaging*. Integr. Biol. , 2010. **2**: p. 121-129.
68. Barman, B. and K.C. Sarma, *Luminescence Properties of ZnS Quantum Dots Embedded in Polymer Matrix*. Chalcogenide Lett. , 2011. **8**(3): p. 171-176.
69. Moreels, I., et al., *Size-Tunable, Bright, and Stable PbS Quantum Dots: A Surface Chemistry Study*. ACS Nano, 2011. **5**(3): p. 2004-2012.
70. Bhattacharya, P., S. Ghosh, and A.D. Stiff-Roberts, *Quantum Dot Opto-Electronic Devices*. Annu. Rev. Mater. Res., 2004. **34**: p. 1-40.
71. Luque, A., A. Marti, and A.J. Nozik, *Solar Cells Based on Quantum Dots: Multiple Exciton Generation and Intermediate Bands*. MRS Bull., 2007. **32**: p. 236-241.
72. Jaiswal, J.K. and S.M. Simon, *Potentials and Pitfalls of Fluorescent Quantum Dots for Biological Imaging*. Trends Cell Biol. , 2004. **14**(9): p. 497-504.
73. Gao, X., et al., *In Vivo Molecular and Cellular Imaging with Quantum Dots*. Curr. Opin. Biotech., 2005. **16**: p. 63-72.
74. Alivisatos, A.P., W. Gu, and C. Larabell, *Quantum Dots as Cellular Probes*. Annu. Rev. Mater. Res., 2005. **7**: p. 55-76.
75. Chung, H. and S. Das, *Functionally Graded Nylon-11/Silica Nanocomposites Produced by Selective laser Sintering*. Mater. Sci. Eng. A, 2008. **487**: p. 251-257.
76. Cai, K., et al., *Direct-Writing Construction of Layered Meshes from Nanoparticles-Vaseline Composite Inks: Rheological Properties and Structures*. Appl. Phys. A, 2011. **102**: p. 501-507.
77. Duan, Y., et al., *Nano-TiO₂-Modified Photosensitive Resin for RP*. Rapid Prototyping J., 2011. **17**(4).
78. Li, Q. and J.A. Lewis, *Nanoparticle Inks for Directed Assembly of Three-Dimensional Periodic Structures*. Adv. Mater., 2003. **15**(19): p. 1639-1643.
79. Zheng, H., et al., *Effect of Core-Shell Composite Particles on the Sintering Behavior and Properties of Nano-Al₂O₃/Polystyrene Composite Prepared by SLS*. Mater. Lett. , 2006. **60**: p. 1219-1223.
80. Duan, B., et al., *Three-Dimensional Nanocomposite Scaffolds Fabricated via Selective Laser Sintering for Bone Tissue Engineering*. Acta Biomater. , 2010. **6**: p. 4495-4505.